SUVmax of FDG PET-CT Can Be Used As An Identifier of Lesion for AI To Interpret Radiology Reports

Kenji Hirata
Hokkaido University
Osamu Manabe (osamumanabe817@med.hokudai.ac.jp)
Hokkaido University Hospital https://orcid.org/0000-0001-8518-8441
Keiichi Magota
Hokkaido University
Sho Furuya
Hokkaido University
Tohru Shiga
Hokkaido University
Kohsuke Kudo
Hokkaido University

Research article

Keywords: Standardized uptake value, SUVmax, Identifier, FDG PET-CT, AI, training data

Posted Date: August 24th, 2020

DOI: https://doi.org/10.21203/rs.3.rs-61799/v1

Abstract

Background Radiology reports contribute not only to the particular patient, but also to constructing massive training dataset in the era of artificial intelligence (AI). The maximum standardized uptake value (SUVmax) is often described in daily radiology reports of FDG PET-CT. If SUVmax can be used as an identifier of lesion, that would greatly help AI interpret radiology reports. We aimed to clarify whether the lesion can be localized using SUVmax written in radiology reports.

Methods The institutional review board approved this retrospective study. We investigated a total of 112 lesions from 30 FDG PET-CT images acquired with 3 different scanners. SUVmax was calculated from DICOM files based on the latest Quantitative Imaging Biomarkers Alliance (QIBA) publication. The voxels showing the given SUVmax were exhaustively searched in the whole-body images and counted. SUVmax was provided with 5 different degrees of precision: integer (e.g., 3), 1st decimal places (DP) (3.1), 2nd DP (3.14), 3rd DP (3.142), and 4th DP (3.1416). For instance, when SUVmax=3.14 was given, the voxels with $3.135 \leq SUVmax < 3.145$ were extracted. We also evaluated whether local maximum restriction could improve the identifying performance, where only the voxels showing the highest intensity within some neighborhood were considered. We defined that “identical detection” was achieved when only single voxel satisfied the criterion.

Results A total of 112 lesions from 30 FDG PET-CT images were investigated. SUVmax ranged from 1.3 to 49.1 (median = 5.6, IQR = 5.2). Generally, when larger and more precise SUVmax values were given, fewer voxels satisfied the criterion. The local maximum restriction was very effective. When SUVmax was determined to 4 decimal places (e.g., 3.1416) and the local maximum restriction was applied, identical detection was achieved in 33.3% (lesions with $SUVmax < 2$), 79.5% ($2 \leq SUVmax < 5$), and 97.8% ($5 \leq SUVmax$) of lesions.

Conclusions SUVmax of FDG PET-CT can be used as an identifier to localize the lesion if precise SUVmax is provided and local maximum restriction was applied, although the lesions showing $SUVmax < 2$ were difficult to identify. The proposed method may have potential to make use of radiology reports retrospectively for constructing training datasets for AI.

Introduction

The clinical usefulness of positron emission tomography (PET) using 18F-fluorodeoxyglucose (FDG) has been well established in oncology [1]. In addition to visual assessment (qualitative analysis), several quantitative measurements have been used to express the degree of FDG uptake. Among them, the standardized uptake value (SUV) has long been used as the de facto standard. To our knowledge, SUV was first extensively used around 1991 [2]. In the initial years of its use, SUV was also known as the differential uptake ratio [3] or dose uptake ratio [4]. The in-lesion maximum of SUV, or SUVmax, has frequently been used since 1999. By 2009 SUVmax had become the most frequently used measurement by far, with 6-fold more frequent use compared to the next most-often used measurement, according to a

comprehensive review [5]. Although SUV is most commonly calculated as the radioactivity concentration normalized to injection dosage and body weight, other definitions include the radioactivity concentration normalized to the body surface area [6], to lean body mass [5], and to blood glucose [7]. While metabolic tumor volume and total lesion glycolysis have been extensively investigated in recent studies [8, 9], SUVmax is still superior to them in terms of its extremely high inter-operator reproducibility. Many lines of evidence have demonstrated the usefulness of SUVmax for differential diagnosis, treatment response prediction, and prognosis [10].

In 2015, 229.2 CT and 113.4 MRI examinations per 1000 population were performed [11]. 42.1 radiologists per million population were employed, and thus 8137 CT/MRI examinations were performed per radiologist [11]. As for nuclear medicine, 0.6 million FDG PET studies were performed in Japan in 2017 [12]. A significant number of these studies require radiologist(s) to interpret the images and write the reports. Describing intensity of FDG uptake either using SUVmax or qualitatively has been recommended [13]. Radiology reports not only contribute greatly to helping the attending physician interpret the image and diagnose the disease, but also prevent important findings from being overlooked. More recently, in the era of artificial intelligence (AI), the importance of training data is increasing. Collectively, radiology reports form a highly useful and efficient training database [14–18].

We hypothesized that if the SUVmax described in radiology reports was sufficiently precise, it might contribute to localization of the lesion, because there should be a limited number of voxels showing the same SUVmax in the entire image. In other words, we thought that SUVmax could be used as an identifier of the lesion. Thus, in this study, we aimed to clarify whether it would be possible to identify the lesion location using the SUVmax under various conditions by varying the degree of SUVmax precision and applying local maximum restriction. Such a technique could also be used to realize an automated system to generate a visual summary of the radiology report (Fig. 1).

Materials And Methods

Study subjects

This retrospective observation study was approved by the institutional review board (approval no. 017-0454). The requirement of written informed consent from each patient was waived because of the study's retrospective nature. We confirmed that all methods were carried out in line with the relevant guidelines and regulations. A total of 30 PET-CT scans (sequential examinations for each scanner) were investigated in this study. No more than one scan was included for each patient. All the images were acquired between April 2019 and November 2019. Images were evaluated visually, and included to the study population if there were any pathological FDG uptakes in visual analysis until the number of scans reached 10 for each scanner. When all the FDG accumulation mass were considered physiological, the case was excluded. Note that not only uptake due to pathological malignancy but also malignancy-suspected and inflammatory uptakes were included in the analysis. In cases in which more than 5

uptakes were found, a maximum of 5 uptakes were recorded for a patient. An experienced nuclear medicine physician visually evaluated all the images.

PET-CT image acquisition and reconstruction

In this study, we investigated images acquired with 3 different PET-CT scanners made by 2 different manufacturers.

Scanner 1 was a Biograph 64 True Point PET-CT (Asahi-Siemens Medical Technologies, Tokyo). The transaxial and axial fields of view were 68.4 cm and 21.6 cm, respectively. Images were reconstructed using the OSEM algorithm with point spread function correction. Time-of-flight of photons was not measurable with the scanner. The reconstructed images had a matrix size of 168 × 168 and a voxel size of 4.1 × 4.1 × 2.0 mm.

Scanner 2 was a GEMINI TF64 PET-CT (Philips Japan, Tokyo). The transaxial and axial fields of view were 57.6 cm and 18.0 cm, respectively. Images were reconstructed using the OSEM algorithm reinforced with the time-of-flight algorithm. Point spread function correction was not applied. The reconstructed images had a matrix size of 144 × 144 and a voxel size of 4.0 × 4.0 × 4.0 mm.

Scanner 3 was a Vereos PET-CT (Philips Japan, Tokyo), which was the newest scanner of the three and equipped with digital photon counting detectors [19]. The transaxial and axial fields of view were 67.6 cm and 16.4 cm, respectively [19]. Images were reconstructed using the OSEM algorithm. Both the time-of-flight algorithm and point spread function correction were applied. The reconstructed images had a matrix size of 256 × 256 and a voxel size of 2.0 × 2.0 × 2.0 mm.

The number of voxels in the z-direction (i.e., cranio-caudal direction) ranged from 234 to 553, resulting in the final number of voxels ranging from 4.85×10^6 to 4.41×10^7. CT images were used for attenuation correction for all the scanners and for visual assessment, but were not analyzed quantitatively in the current study. All patients fasted for ≥ 6 hours before the injection of FDG (approx. 4 MBq/kg), and the emission scanning was initiated basically around 60 min post-injection. One scan was acquired 95 min post-injection due to mechanical troubles. Fasting blood sugar was confirmed to be smaller than 200 mg/dl in each study.

SUVmax calculation

Commercially available DICOM viewers / PET viewers do not display SUVmax to 4 decimal places (DP) or higher. In order to obtain the ground truth of SUVmax, we modified Metavol software package, which we previously developed for PET-CT volumetric analysis [20]. We used Windows 10, Microsoft Visual Studio Community 2019 Version 16.4.0, C# 8.0 language, .NET Core 3.1, and fo-dicom 4.0.3 for modifying Metavol. For instance, in the case that the true SUVmax is 3.14159, the modified Metavol will display it as it is, whereas XTREK VIEW software (J-MAC SYSTEM, Sapporo, Japan) will display it as 3.142. A nuclear

medicine physician measured SUVmax by placing a spherical volume of interest (VOI) whose diameter can be changed by the operator.

After the VOI definition, SUVmax was calculated based on the newest QIBA publication [21]. Briefly, in Biograph64 and Vereos, the radioactivity concentration c (Bq/ml) was calculated as follows:

$c = \rho \times s + i$.

Here, ρ represents the raw pixel value that was stored with DICOM tag of (7FE0,0010) with each voxel expressed in a 16-bit integer. s represents the *rescale slope*, which is stored as a float value at (0028,1053). i represents the *rescale intercept*, which is stored as a float value at (0028,1052). Next, decay-corrected injection dosage D_c was calculated as follows:

$D_c = D_0 \times (1/2)^{(Ta - Ti)/h}$.

Here, D_0 represents the *radionuclide total dose* (i.e., injected dosage of FDG) (Bq) stored as a float value at (0018,1074). T_a represents *acquisition time* stored at (0008,0032). T_i represents the *radiopharmaceutical start time* (i.e., injection time) stored at (0018,1072). Both times are stored in a "hhmmss" form string, and thus conversion to second is needed. h represents the *radionuclide half-life* (second) stored as a float value at (0018,1075).

Finally, SUV was calculated as follows:

$SUV = c \times w / D_c$.

Here, w represents the *patient's weight* (g), which is stored in kilograms at (0010,1030) and thus must be multiplied by 1000.

The SUV calculation was much simpler in GEMINI TF64, as follows:

$SUV = (\rho \times s + i) \times p$.

Here, p represents the *Philips Factor* (float) stored as a float value at (7053, 1000). The values of s and i were 1 and 0, respectively, for all the GEMINI TF64 examinations investigated in the current study.

Lesion localization

We implemented a function that searches voxels satisfying the given SUV range and illustrate the locations in the whole body image (Figs. 2-4). The SUV range was determined as follows. When "3" was provided by the operator, the range was considered to be $2.5 \leq SUV < 3.5$. When "3.1" was provided, the voxels satisfying $3.05 \leq SUV < 3.15$ were picked out, and so forth. Thus, the more precise the provided value of SUVmax (i.e., more digits) was, the narrower the range of SUV applied to extract voxels was. We compared the results from integer precision to 4th DP precision. Note that we do not show the results of

5th DP precision because there were no cases in which 5th DP precision improved the identification rate compared to 4th DP precision.

We performed experiments in different settings. First, the voxels within the range were extracted simply. Then, local maximum restriction was added to discard the voxel that was adjacent to the higher-value voxel, because such a voxel cannot have SUVmax. For local maximum restriction, milder restriction and stricter restriction were tested. Milder restriction was a condition under which the voxel must be highest in the 3×3×3 cube. Stricter restriction was a condition under which the voxel must be highest in the 5×5×5 cube.

Here, we defined that “identical detection” was achieved when only 1 voxel satisfied the criterion.

Statistical analysis

The relationship between SUVmax vs. the number of voxels detected (N) was estimated using Pearson’s correlation coefficient of the log of SUVmax vs. the log of N. The effects of the precision of SUVmax, i.e., the number of digits after the decimal point, and local maximum restriction on the rate of identical detection were tested using a chi-square test. P values less than 0.05 were considered statistically significant.

Results

Patient characteristics are summarized in Table 1. Diagnosis and lesion locations are summarized in Table 2. In this study population, head-and-neck cancer was the most common diagnosis, and the mediastinal and hilar lymph nodes were the most frequent locations. In the 112 lesions investigated, SUVmax ranged from 1.3 to 49.1, with median and IQR values of 5.6 and 5.2, respectively. SUVmax was significantly higher for Vereos than for Biograph64 and TF64 ($P < 0.01$ and $P < 0.05$, respectively; Supplementary Fig. 1). The numbers of lesions for Biograph64, GEMINI TF64, and Vereos were 37, 37, and 38, respectively.

Table 1
Patient characteristics

	Minimum	25-percentile	50-percentile (median)	75-percentile	Maximum
Age (year)*	11	62.25	69	75	86
Body weight (kg)	35.6	50.75	54.5	65.7	78.5
Fasting blood sugar (mg/dl)**	82	92.25	100.5	107	182
Fasting time (hour)	6.5	8.125	16.5	18	23
Uptake time (min)***	53	55	56	60.5	95
*1 (3%) patient was younger than 20 years old.					
**4 (13%) patients were diagnosed as having diabetes.					
*** Time duration between FDG injection and image acquisition start.					

Table 2
Diagnosis and lesion sites

Diagnosis	Number of patients	Site	Number of lesions
Head and neck cancer	11	Mediastinal and hilar nodes	29
Lung cancer	5	Bone	20
Colorectal cancer	4	Neck and subclavian nodes	17
Malignant lymphoma	2	Lung	16
Primary unknown cancer	2	Abdominal nodes	6
Spinal cord tumor	2	Nasal cavity and pharynx	4
Myelitis	1	Intestine	4
Hepatobiliary cancer	1	Breast	3
Mediastinal tumor	1	Spinal cord	3
Sarcoidosis	1	Other soft tissues	3
		Axillary nodes	2
		Liver	1
		Inguinal nodes	1
		Adrenal gland	1
		Parotid gland	1
		Peripheral nerve	1
Total	30		112

First, local maximum restriction was not applied. A number of voxels were identified corresponding to the given SUVmax (Fig. 5, top row). Generally, when a larger SUVmax was given, a smaller number of voxels was detected ($0.83<|r|<0.84$, $P < 10^{-28}$). When the SUVmax was given with 10-fold greater precision, an approximately 0.1-fold number of voxels were extracted, as expected theoretically.

Next, local maximum restriction was applied. Both $3 \times 3 \times 3$ and $5 \times 5 \times 5$ local maximum restriction reduced the number of extracted voxels up to 1/1000 (Fig. 5, middle and bottom rows). More specifically, the rate of identical detection increased when the given SUVmax was more precise and local maximum restriction was stricter (Fig. 6). For instance, while identical detection was successful only in 2.7% of patients when integer precision and no restriction were used, the success rate was elevated to 86.6%

when 4th DP precision and 5 × 5 × 5 local maximum restriction were used. The effects of 5 × 5 × 5 over 3 × 3 × 3 local maximum restriction were observed as shown in Fig. 6, except for integer precision, although none of the differences between 5 × 5 × 5 vs. 3 × 3 × 3 local maximum restriction reached the level of statistical significance ($P > 0.05$).

For sub-analysis, all lesions were categorized as low (SUVmax < 2, N = 6), medium (2 ≤ SUVmax < 5, N = 44), or high (5 ≤ SUVmax, N = 62) uptake lesions. The rate of identical detection was low (33.3%) for the low uptake group even under the best conditions, although the medium (79.5%) and high (96. 8%) uptake groups achieved high rates (Fig. 7). To investigate the underlying mechanisms for this difference, we drew a histogram of SUV over the whole-body image of a patient (Fig. 8). In this case, the frequency exponentially decreased when SUVmax increased, as 98.13% of voxels showed 0 ≤ SUV < 1, 1.28% showed 1 ≤ SUV < 2, 0.37% showed 2 ≤ SUV < 5, and 0.21% showed 5 ≤ SUV.

Discussion

In this retrospective study, we aimed to clarify whether SUVmax can be used as a lesion identifier to localize the voxel in the whole-body image of FDG PET. We observed that SUVmax successfully localized the voxel for > 80% examinations in the case that SUVmax was given to the 3rd or higher DP and local maximum restriction (5 × 5 × 5) was applied. However, the sub-analysis showed that the lesions having SUVmax < 2 were difficult to localize using SUVmax only. To our knowledge, this is the first report to show the use of SUVmax as an identifier of lesion on FDG PET-CT.

The pixel data was stored in DICOM files in a 16-bit integer form for all 3 scanners investigated. A 16-bit integer can express 65,536 different values. Since the number of voxels in the whole-body image may be around 10^7, theoretically > 100 voxels on average may have exactly the same value. In fact, however, the distribution of SUV was quite skewed, as shown in Fig. 8. It is reasonable that many voxels were detected when a smaller SUVmax was given, whereas only single voxel was detected when a larger SUV (e.g. >5) was given. In Fig. 5, the number of voxels suddenly dropped once SUVmax became larger than 10. This can be explained as follows. In this study, we used DP instead of significant figures. They are slightly but clearly different. DP means the number of digits located to the right of the decimal point. Significant figures refers to the total number of digits irrespective of the decimal point location. For example, 9.8 is 1st DP and 2 significant figures, whereas 12.3 is 1st DP and 3 significant figures. Since 12.3 has more information than 9.8, fewer voxels were included within the range.

The effect of local maximum restriction was significant. The number of voxels that can become local maxima depends on the noise level of the image. Mathematically, when 3 × 3 × 3 restriction was applied, at most 1 of 2 voxels in each axis could become local maxima, indicating that 1/8 or a smaller number of voxels could become local maxima. Similarly, when 5 × 5 × 5 restriction was applied, at most 1 of 3 voxels in each axis and thus 1/27 or a smaller number of voxels could become local maxima. We did not try 7 × 7 × 7 restriction because we were worried that it might prevent identification of the voxel of SUVmax,

considering that a single voxel size is 4 mm, and its diagonal is $4\sqrt{3} = 6.9$ mm, and thus 7 voxels account for as large as 48.5 mm.

Some may argue that use of the 3rd or higher DP for SUVmax is redundant for daily radiological reports. That is true. SUV calculation uses body weight and the precision of body weight measurement may be 3 significant figures (e.g., 56.7 kg) or less. Radioactivity dosage measurements may introduce some errors. Furthermore, SUV varies depending on various technical (e.g., scanner, acquisition protocol, reconstruction protocol) and physiological (e.g., fasting conditions) factors. Therefore, the number excessive fine number is meaningless in diagnosis and treatment planning. Those may be why SUVmax is often written to the 1st DP (e.g., 3.1). However, in order to permit the future use of SUVmax as an identifier, we would like to propose that SUVmax be written as precisely as the PET-CT viewer allows. As mentioned before, this use of SUVmax would allow the radiology report to be summarized as a single image (Fig. 1). In addition, it may also help radiologists to locate a lesion mentioned in a previous report so as to compare between past and present images. Our ultimate goal is to build a massive training dataset based on radiology reports and corresponding images. Writing the coordinate values (x,y,z) in the reports will be the best way to transfer the information to artificial intelligence. Currently, that may not be possible in most viewers and reporting systems. Also, the appearance of such information in the middle of a report may distract readers, and thus an automated system is needed to hide this information when humans read the report.

The use of SUVmax is specific for PET. Although the maximum voxel value may not often be useful for CT or MRI, the idea could be applied to the apparent diffusion coefficient (ADC) images derived from diffusion weighted imaging of MRI, because the minimum of ADC is meaningful for diagnosis.

As limitations of the current study, we did not investigate the SUVmax shown in different image viewers. In some viewers, PET volumes are reconstructed (resliced) in the CT alignment, making slight changes to SUVmax. Second, we did not directly use the radiology reports but reviewed the images to re-measure SUVmax. Thus, we could not estimate the number of actual cases in which the SUVmax written in the reports could successfully locate the lesion. Such a study needs to be carried out. Third, head and neck cancer accounted for a large portion of the current study population, which does not necessarily reflect general population undergoing PET-CT. Finally, radiology reports often provide anatomical terms in the same sentence with SUVmax. This would be great information for selecting the appropriate location when SUVmax suggests several candidates, as in Fig. 3. Such a method will be tested in future studies.

Conclusion

The data suggested that SUVmax can be used as an identifier of lesion on FDG PET-CT. For this purpose, it is important that SUVmax is given precisely (3rd DP or more) and that local maximum restriction is applied to identify the voxel. The lesions showing SUVmax < 2 were difficult to identify. The proposed method may have potential to make use of radiology reports retrospectively for constructing training datasets for AI.

Abbreviations

DP: decimal places; FDG: fluorodeoxyglucose; OSEM: ordered subsets expectation maximization; QIBA: Quantitative Imaging Biomarkers Alliance; SUV: standardized uptake value; VOI: volume of interest

Declarations

Acknowledgments

We thank all staff in the nuclear medicine department of our hospital.

Authors' contributions

KH and OS designed experiments, performed experiments, wrote and revised the manuscript. KM and SF collected image data. TS and KK wrote and revised the manuscript. All authors read and approved the

final manuscript.

Funding

This work was supported by JST COI Grant Number JPMJCE1301 (H31W09).

Availability of data and materials

The datasets used and/or analyzed during the current study are available from the corresponding author on reasonable request. Anyone who is interested in the information should contact Osamu Manabe.

Ethics approval and consent to participate

All procedures performed in this study involving human participants were in accordance with the ethical standards of the institutional review board (017-0454) and with the 1964 Helsinki Declaration and its later amendments or comparable ethical standards (EudraCT nr, 2017-003461-96).

Consent for publication

Not applicable

Competing interests

The authors declare that they have no competing interests.

References

1. Ben-Haim S, Ell P. 18F-FDG PET and PET/CT in the evaluation of cancer treatment response. J Nucl Med. 2009;50:88-99. doi:10.2967/inumed.108.054205.

2. Haberkorn U, Strauss LG, Dimitrakopoulou A, Engenhart R, Oberdorfer F, Ostertag H, et al. PET studies of fluorodeoxyglucose metabolism in patients with recurrent colorectal tumors receiving radiotherapy. J Nucl Med. 1991;32:1485-90.
3. Griffeth LK, Dehdashti F, McGuire AH, McGuire DJ, Perry DJ, Moerlein SM, et al. PET evaluation of soft-tissue masses with fluorine-18 fluoro-2-deoxy-D-glucose. Radiology. 1992;182:185-94. doi:10.1148/radiology.182.1.1727280.
4. Adler LP, Blair HF, Makley JT, Williams RP, Joyce MJ, Leisure G, et al. Noninvasive grading of musculoskeletal tumors using PET. J Nucl Med. 1991;32:1508-12.
5. Wahl RL, Jacene H, Kasamon Y, Lodge MA. From RECIST to PERCIST: Evolving Considerations for PET response criteria in solid tumors. J Nucl Med. 2009;50 Suppl 1:122s-50s. doi:10.2967/jnumed.108.057307.
6. Kim CK, Gupta NC, Chandramouli B, Alavi A. Standardized uptake values of FDG: body surface area correction is preferable to body weight correction. J Nucl Med. 1994;35:164-7.
7. Nozawa A, Rivandi AH, Kesari S, Hoh CK. Glucose corrected standardized uptake value (SUVgluc) in the evaluation of brain lesions with 18F-FDG PET. Eur J Nucl Med Mol Imaging. 2013;40:997-1004. doi:10.1007/s00259-013-2396-9.
8. Kitao T, Shiga T, Hirata K, Sekizawa M, Takei T, Yamashiro K, et al. Volume-based parameters on FDG PET may predict the proliferative potential of soft-tissue sarcomas. Ann Nucl Med. 2019;33:22-31. doi:10.1007/s12149-018-1298-0.
9. Kitao T, Hirata K, Shima K, Hayashi T, Sekizawa M, Takei T, et al. Reproducibility and uptake time dependency of volume-based parameters on FDG-PET for lung cancer. BMC Cancer. 2016;16:576. doi:10.1186/s12885-016-2624-3.
10. Krak NC, Boellaard R, Hoekstra OS, Twisk JW, Hoekstra CJ, Lammertsma AA. Effects of ROI definition and reconstruction method on quantitative outcome and applicability in a response monitoring trial. Eur J Nucl Med Mol Imaging. 2005;32:294-301. doi:10.1007/s00259-004-1566-1.
11. Kumamaru KK, Machitori A, Koba R, Ijichi S, Nakajima Y, Aoki S. Global and Japanese regional variations in radiologist potential workload for computed tomography and magnetic resonance imaging examinations. Jpn J Radiol. 2018;36:273-81. doi:10.1007/s11604-018-0724-5.
12. Nishiyama Y, Kinuya S, Kato T, Kayano D, Sato S, Tashiro M, et al. Nuclear medicine practice in Japan: a report of the eighth nationwide survey in 2017. Ann Nucl Med. 2019;33:725-32. doi:10.1007/s12149-019-01382-5.
13. Niederkohr RD, Greenspan BS, Prior JO, Schoder H, Seltzer MA, Zukotynski KA, et al. Reporting guidance for oncologic 18F-FDG PET/CT imaging. J Nucl Med. 2013;54:756-61. doi:10.2967/jnumed.112.112177.
14. Dalal S, Hombal V, Weng WH, Mankovich G, Mabotuwana T, Hall CS, et al. Determining Follow-Up Imaging Study Using Radiology Reports. J Digit Imaging. 2019. doi:10.1007/s10278-019-00260-w.
15. Liu Y, Liu Q, Han C, Zhang X, Wang X. The implementation of natural language processing to extract onance imaging reports. BMC medical informatics and

decision making. 2019;19:288. doi:10.1186/s12911-019-0997-3.

16. Spandorfer A, Branch C, Sharma P, Sahbaee P, Schoepf UJ, Ravenel JG, et al. Deep learning to convert unstructured CT pulmonary angiography reports into structured reports. European radiology experimental. 2019;3:37. doi:10.1186/s41747-019-0118-1.
17. Piotrkowicz A, Johnson O, Hall G. Finding relevant free-text radiology reports at scale with IBM Watson Content Analytics: a feasibility study in the UK NHS. Journal of biomedical semantics. 2019;10:21. doi:10.1186/s13326-019-0213-5.
18. Banerjee I, Bozkurt S, Caswell-Jin JL, Kurian AW, Rubin DL. Natural Language Processing Approaches to Detect the Timeline of Metastatic Recurrence of Breast Cancer. JCO clinical cancer informatics. 2019;3:1-12. doi:10.1200/cci.19.00034.
19. Nguyen NC, Vercher-Conejero JL, Sattar A, Miller MA, Maniawski PJ, Jordan DW, et al. Image Quality and Diagnostic Performance of a Digital PET Prototype in Patients with Oncologic Diseases: Initial Experience and Comparison with Analog PET. J Nucl Med. 2015;56:1378-85. doi:10.2967/jnumed.114.148338.
20. Hirata K, Kobayashi K, Wong KP, Manabe O, Surmak A, Tamaki N, et al. A Semi-Automated Technique Determining the Liver Standardized Uptake Value Reference for Tumor Delineation in FDG PET-CT. PLoS One. 2014;9:e105682. doi:10.1371/journal.pone.0105682.
21. FDG-PET/CT Technical Committee. FDG-PET/CT as an Imaging Biomarker Measuring Response to Cancer Therapy, Quantitative Imaging Biomarkers Alliance, Version 1.13, November 18, 2016. Technically Confirmed Version. http://qibawiki.rsna.org/images/1/1f/QIBA_FDG-PET_Profile_v113.pdf. RSNAORG/QIBA.

Figures

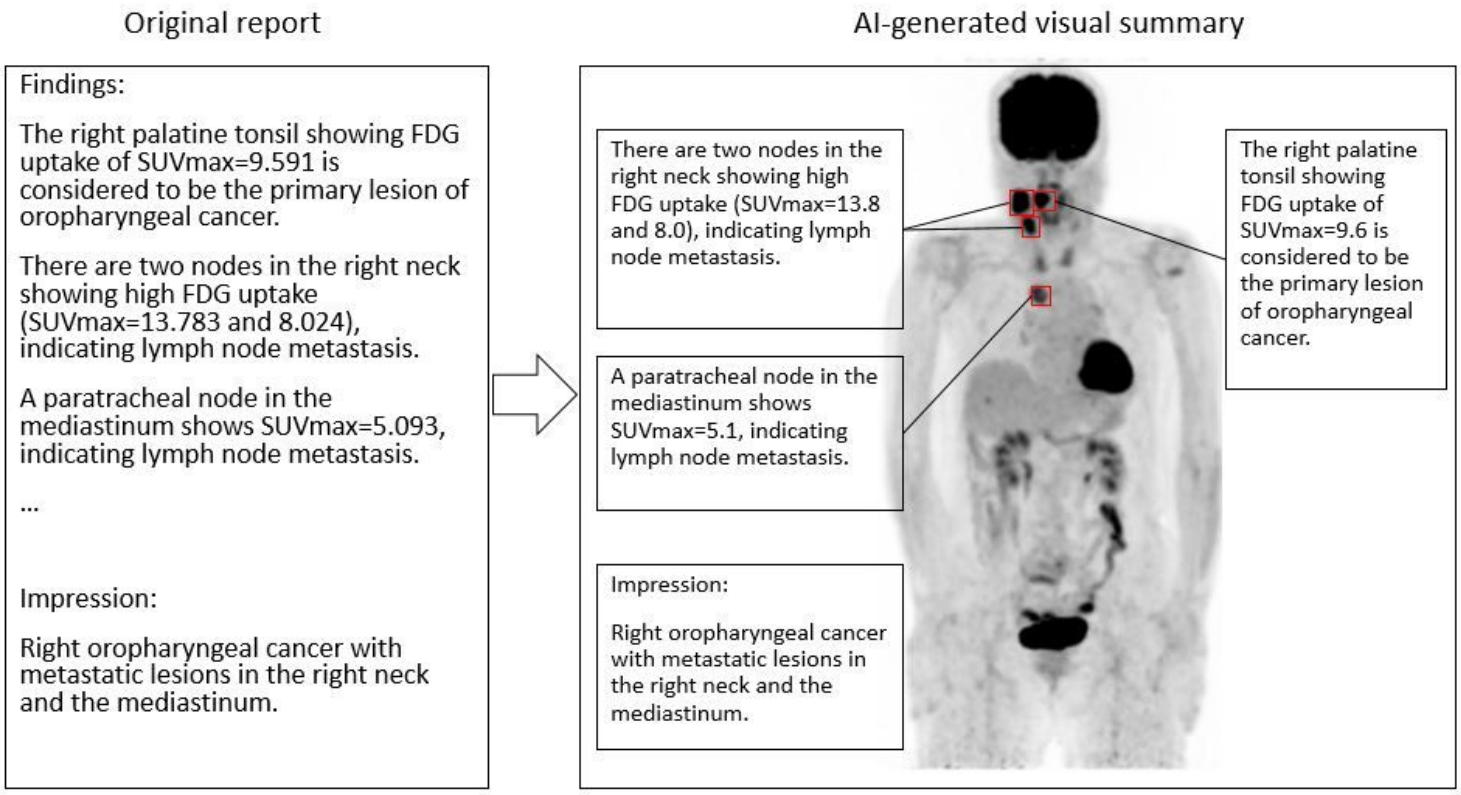

Figure 1

A conceptual image of AI generating the visual summary of the report of FDG PET. SUVmax in the sentence appearing in the report text is used for localization. In this case, the primary lesion (right palatine tonsil) and metastatic nodes show high FDG uptakes. Note that SUVmax should be round before attending physicians read the report.

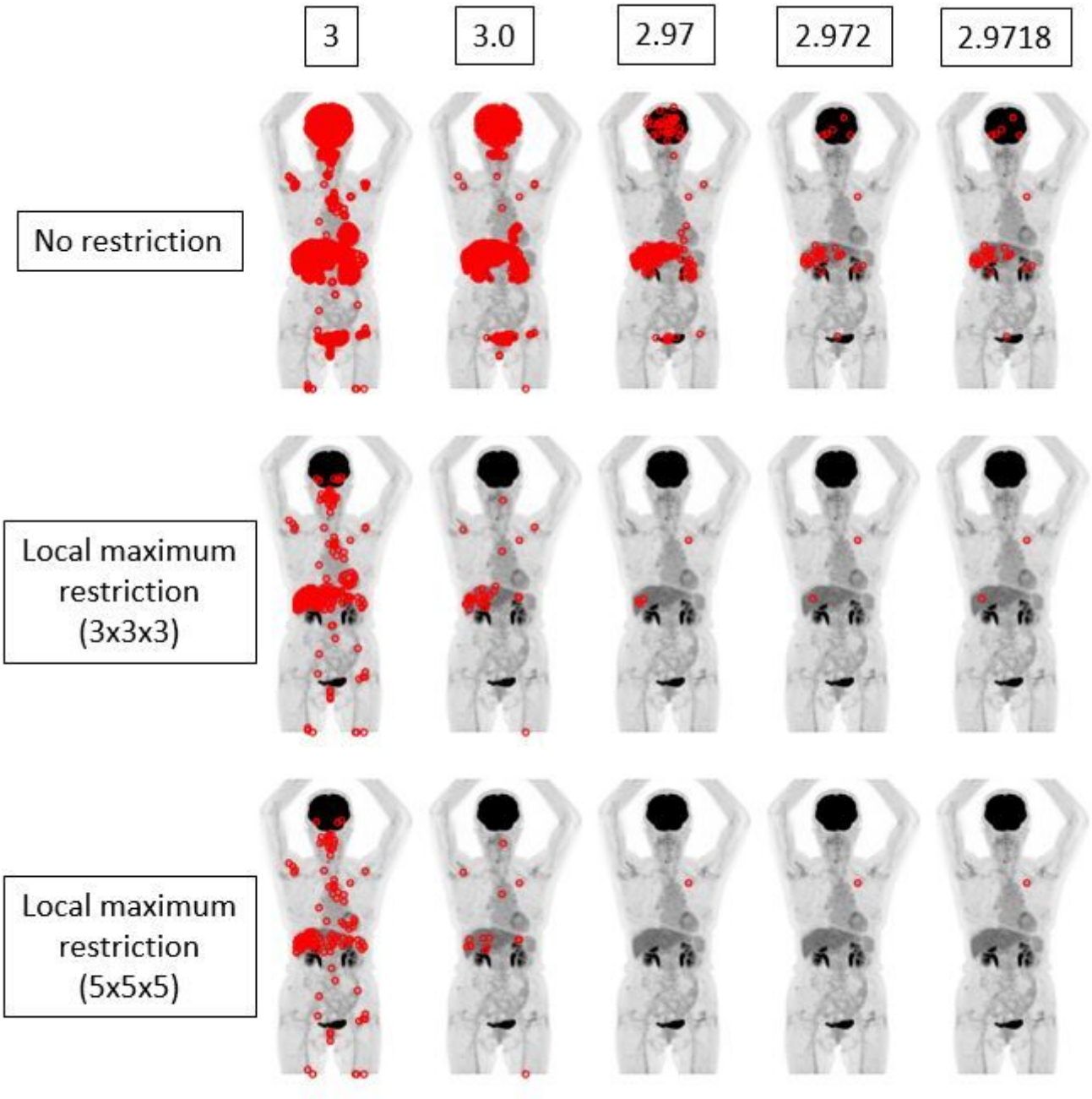

Figure 2

The findings for a patient who underwent FDG PET-CT for lung nodules. The true SUVmax of the nodule in the left upper lobe was 2.97177. When local maximum restriction was not applied, 21031, 2176, 210, 33, and 33 voxels were extracted for 3, 3.0, 2.97, 2.972, and 2.9718, respectively. When 3×3×3 local maximum restriction was applied, 254, 32, 4, 2, and 2 voxels were extracted. When 5×5×5 local maximum restriction was applied, 126, 14, 1, 1, and 1 voxel(s) were extracted, achieving identical detection.

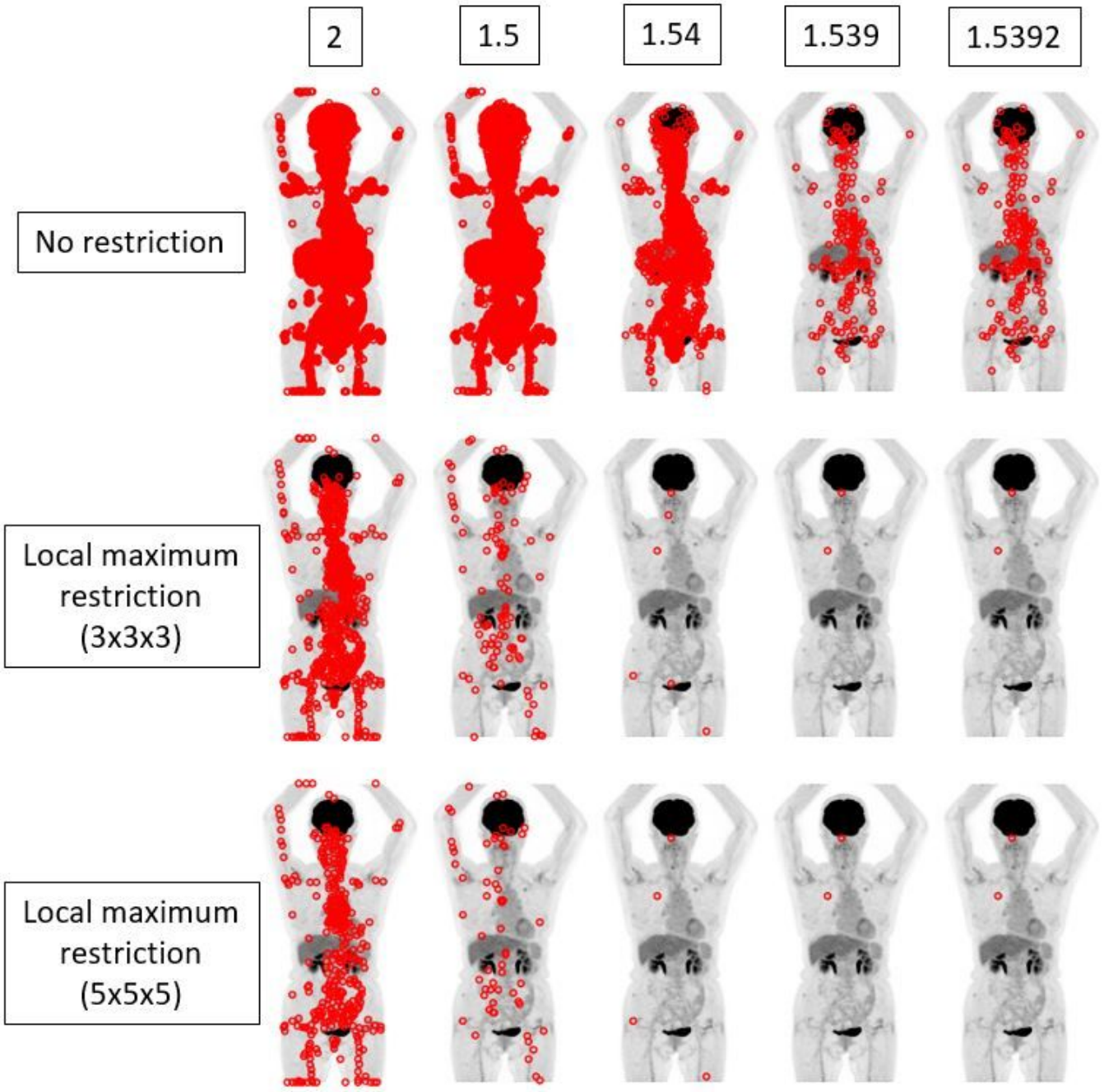

Figure 3

The same case as depicted in Fig. 2. The true SUVmax of the nodule in the right upper lobe was 1.53924. When local maximum restriction was not applied, 74952, 13442, 1427, 198, and 198 voxels were extracted for 2, 1.5, 1.54, 1.539, and 1.5392, respectively. When 3×3×3 local maximum restriction was applied, 782, 104, 6, 2, and 2 voxels were extracted. When 5×5×5 local maximum restriction was applied, 410, 60, 4, 2, and 2 voxels were extracted. Thus, identical detection was not achieved for this lesion.

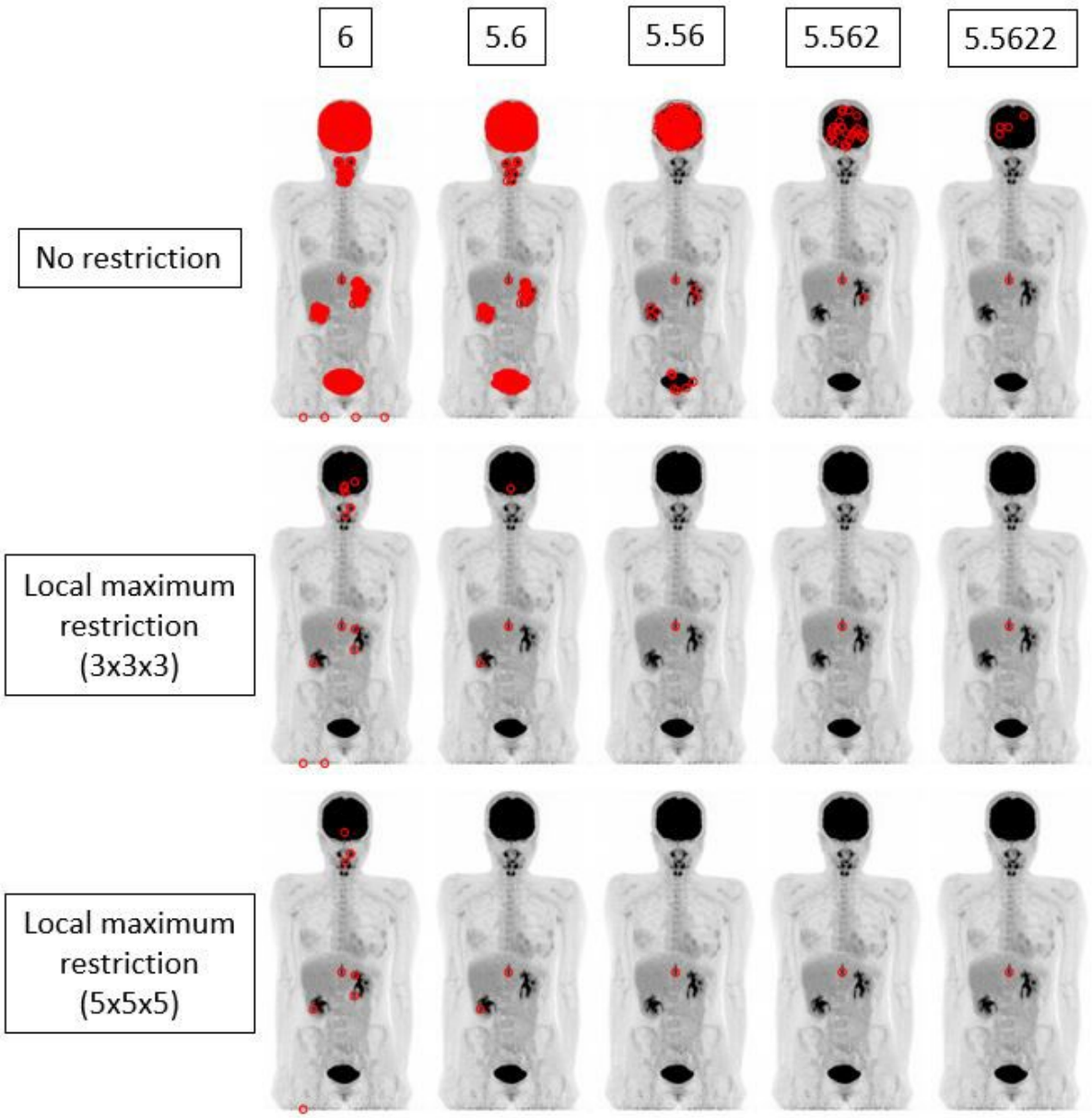

Figure 4

The findings for a patient who underwent FDG PET-CT for a spinal code lesion. The true SUVmax of the nodule in the spinal code lesion was 5.56218. When local maximum restriction was not applied, 21116, 1953, 186, 25, and 5 voxels were extracted for 6, 5.6, 5.56, 5.562, and 5.5622, respectively. When 3×3×3 local maximum restriction was applied, 12, 3, 1, 1, and 1 voxel(s) were extracted. When 5×5×5 local maximum restriction was applied, 8, 2, 1, 1, and 1 voxel(s) were extracted, achieving identical detection.

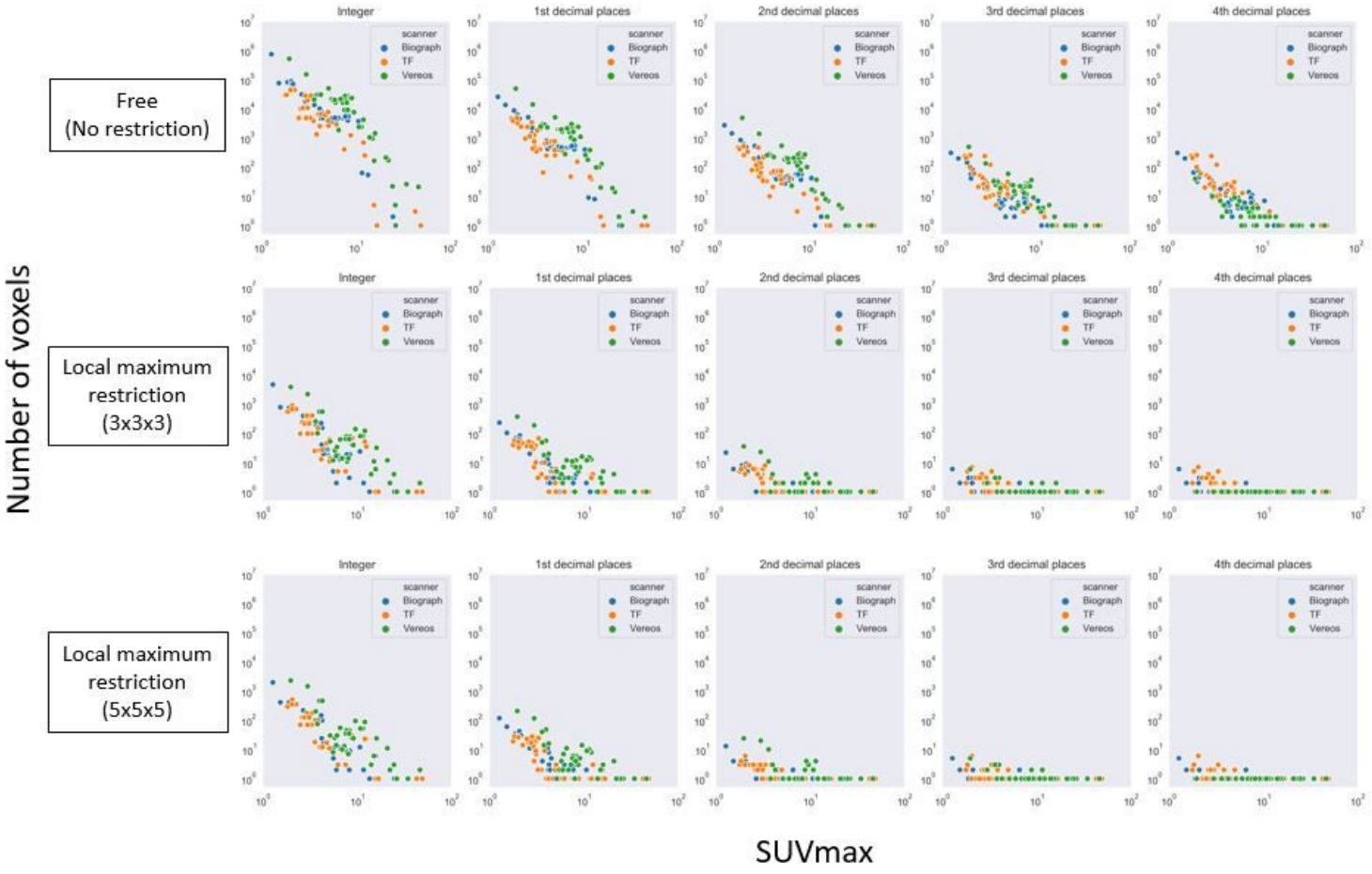

Figure 5

The number of voxels extracted by a given SUVmax with various levels of precision. Top row, local maximum restriction was not applied; middle row, 3x3x3 local maximum restriction was applied; bottom row, 5x5x5 local maximum restriction was applied.

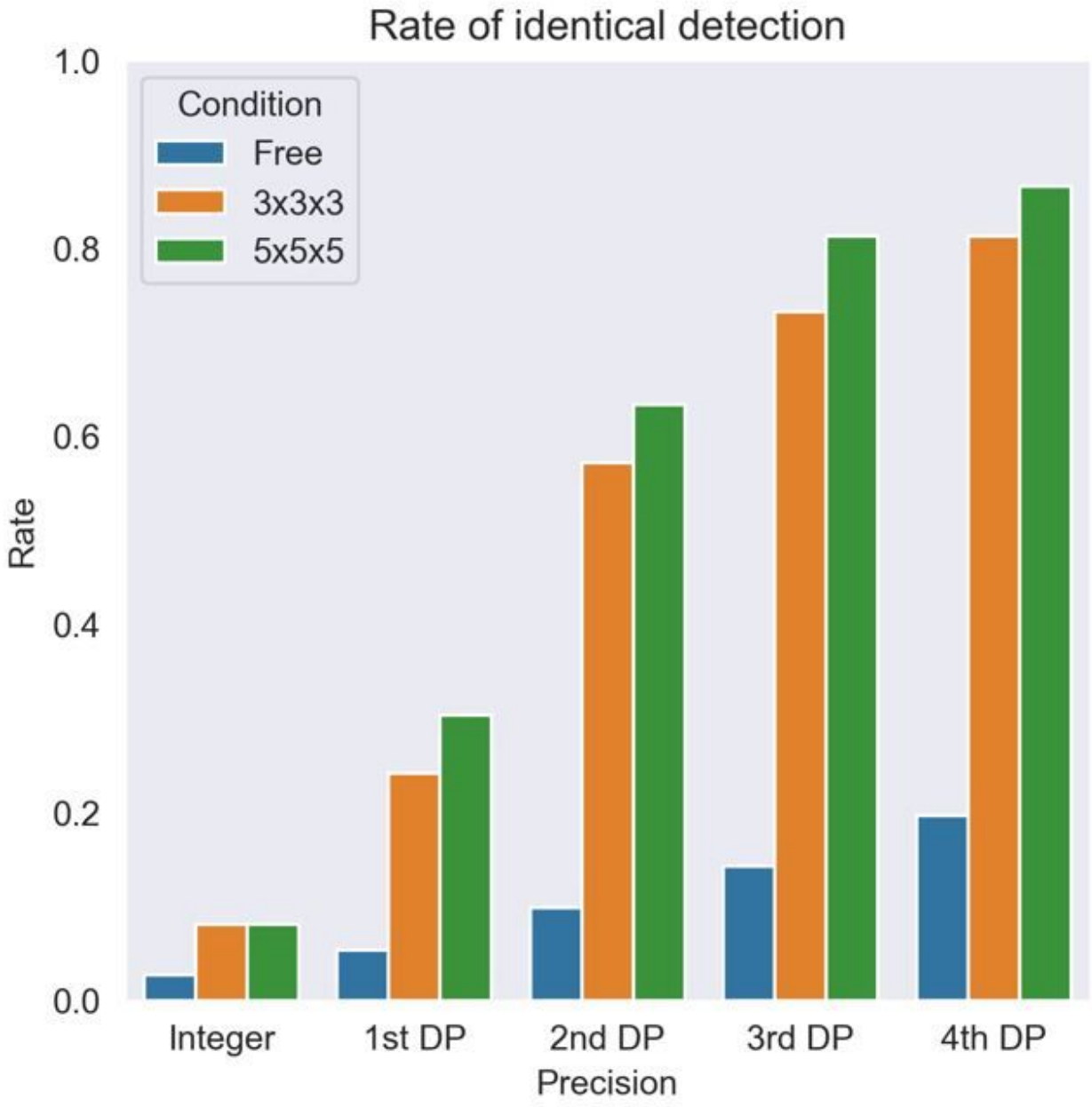

Figure 6

The overall rate of identical detection of the lesion. DP = decimal places. Free, 3×3×3, and 5×5×5 express no restriction and each local maximum restriction.

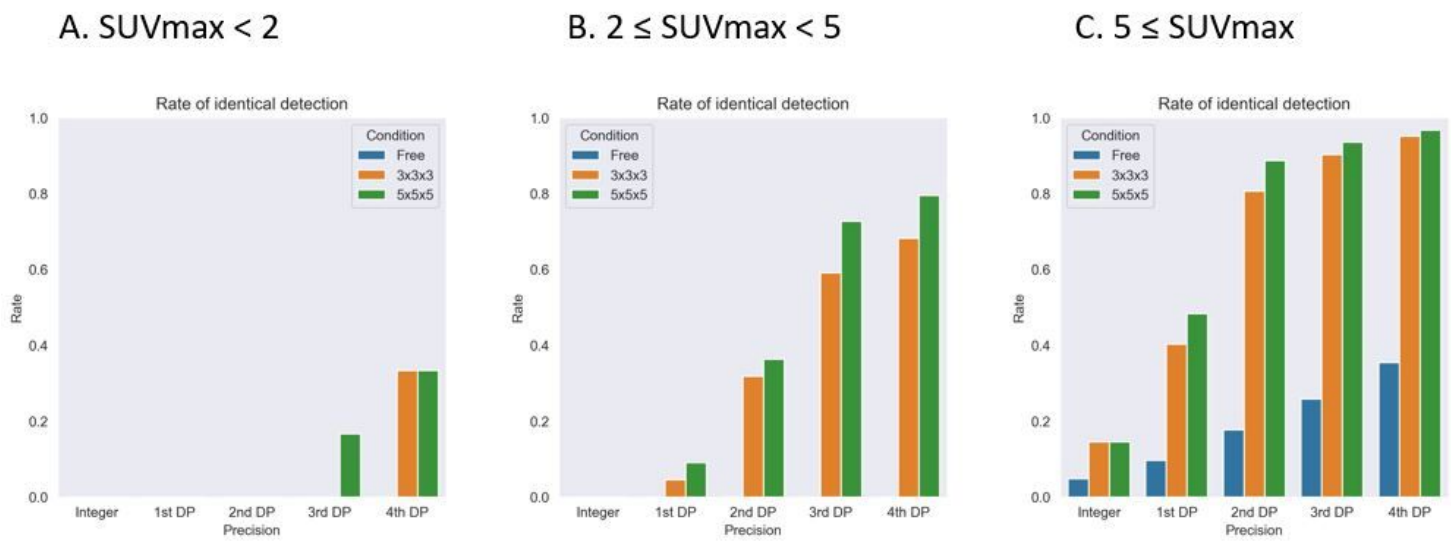

Figure 7

The results of sub-group analysis of the rate of identical detection of the lesions with SUVmax<2 (A, N=6), 2<SUVmax<5 (B, N=44), and 5<SUVmax (C, N=62). DP = decimal places. Free, 3×3×3, and 5×5×5 express no restriction and each local maximum restriction.

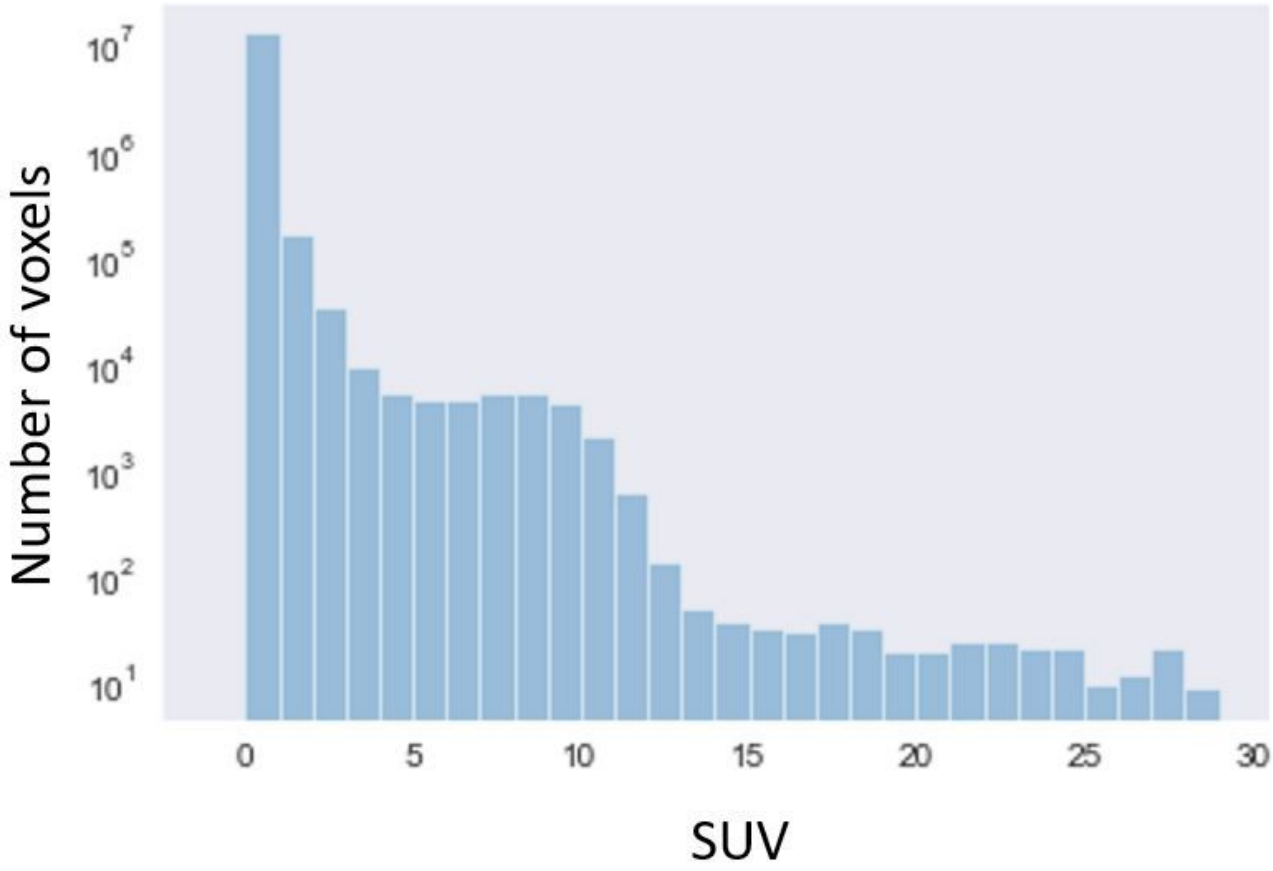

Figure 8

A histogram of SUV over the whole-body image of a patient (semi-log plot).

Supplementary Files

This is a list of supplementary files associated with this preprint. Click to download.

- Supl20200817.pptx